ARTICLE

Check for updates

SH3- and actin-binding domains connect ADNP and SHANK3, revealing a fundamental shared mechanism underlying autism

Yanina Ivashko-Pachima[1,2], Maram Ganaiem[1,2], Inbar Ben-Horin-Hazak[1,2], Alexandra Lobyntseva[1,2], Naomi Bellaiche[1,2], Inbar Fischer[2], Gilad Levy[2], Shlomo Sragovich[1,2], Gidon Karmon[1,2], Eliezer Giladi[1,2], Shula Shazman[3], Boaz Barak[2,4] and Illana Gozes[1,2]✉

De novo heterozygous mutations in activity-dependent neuroprotective protein (ADNP) cause autistic ADNP syndrome. ADNP mutations impair microtubule (MT) function, essential for synaptic activity. The ADNP MT-associating fragment NAPVSIPQ (called NAP) contains an MT end-binding protein interacting domain, SxIP (mimicking the active-peptide, SKIP). We hypothesized that not all *ADNP* mutations are similarly deleterious and that the NAPV portion of NAPVSIPQ is biologically active. Using the eukaryotic linear motif (ELM) resource, we identified a Src homology 3 (SH3) domain-ligand association site in NAP responsible for controlling signaling pathways regulating the cytoskeleton, namely NAPVSIP. Altogether, we mapped multiple SH3-binding sites in ADNP. Comparisons of the effects of ADNP mutations p.Glu830synfs*83, p.Lys408Valfs*31, p.Ser404* on MT dynamics and Tau interactions (live-cell fluorescence-microscopy) suggested spared toxic function in p.Lys408Valfs*31, with a regained SH3-binding motif due to the frameshift insertion. Site-directed-mutagenesis, abolishing the p.Lys408Valfs*31 SH3-binding motif, produced MT toxicity. NAP normalized MT activities in the face of all ADNP mutations, although, SKIP, missing the SH3-binding motif, showed reduced efficacy in terms of MT-Tau interactions, as compared with NAP. Lastly, SH3 and multiple ankyrin repeat domains protein 3 (SHANK3), a major autism gene product, interact with the cytoskeleton through an actin-binding motif to modify behavior. Similarly, ELM analysis identified an actin-binding site on ADNP, suggesting direct SH3 and indirect SHANK3/ADNP associations. Actin co-immunoprecipitations from mouse brain extracts showed NAP-mediated normalization of Shank3-Adnp-actin interactions. Furthermore, NAP treatment ameliorated aberrant behavior in mice homozygous for the *Shank3* ASD-linked InsG3680 mutation, revealing a fundamental shared mechanism between ADNP and SHANK3.

Molecular Psychiatry (2022) 27:3316–3327; https://doi.org/10.1038/s41380-022-01603-w

INTRODUCTION

Activity-dependent neuroprotective protein (ADNP) is vital for brain development and function [1, 2], with deficiencies in ADNP being linked with neurodegenerative/psychiatric diseases [3, 4]. Whole exome sequencing on large cohorts of autism spectrum disorder (ASD) families identified ADNP as a recurrent de novo mutated gene [5–7] associated with a high effect risk and correlation with lower IQ [8]. *ADNP* is estimated to be mutated in at least 0.17% of ASD cases, making it one of the most frequent ASD genes known [5]. More than 30 different *ADNP* mutations with variable expressivity have been found in ADNP syndrome [6]. Interestingly, *ADNP* somatic mutations, possibly accumulating with aging, have also been discovered in post-mortem Alzheimer's disease brains [4]. *ADNP* mutations are thought to trigger ASD pathology via impaired transcription factor activity or participation in the chromatin-remodeling complexes SWI/SNF [5, 9] and ChAHP during embryonic development [10]. Indeed, ADNP regulates hundreds of genes [2, 11], including those of the WNT signaling pathway [12–14], and buffers CCCTC-binding factor (CTCF) interaction sites to maintain three-dimensional chromatin organization [15]. ADNP also contributes to histone acetylation [16] and methylation [17], while associating with prominent regulatory proteins, such as SIRT1 [17] and POGZ [18], targeting epigenetic/transcriptional control.

At the same time, the well-studied coupling of cytoplasmic ADNP to cytoskeletal microtubules (MTs) and MT-associated proteins (e.g., the MT lattice-binding protein Tau and MT end-binding (EB1 and EB3) proteins, representing a sub-family of plus-end tracking proteins (+TIPs)) [19, 20], is also directly associated with the ASD phenotype. It was previously found that heterozygous *Adnp*$^{+/-}$ mice exhibit tauopathy-like features and that the eight amino acid-long peptide NAP (NAPVSIPQ), corresponding to the smallest active fragment of ADNP, protects against ADNP deficiencies [21]. Specifically, NAP prevents MT-related toxicities [20], directly associating with EB1/EB3 proteins through its SxIP motif [19], while recruiting ADNP and other SxIP-containing TIPs to MT growing ends, thus normalizing MT dynamics [11, 19]. We have further proven that EB proteins and Tau expression are required for the protective activity of NAP [19, 20]. NAP enhances Tau-EB protein-MT and Tau-EB protein interactions and impacts MT-based processes associated with Tau and EB proteins, such as

[1]The Elton Laboratory for Neuroendocrinology, Department of Human Molecular Genetics and Biochemistry, Sackler Faculty of Medicine, Adams Super Center for Brain Studies, Tel Aviv University, Tel Aviv, Israel. [2]Sagol School of Neuroscience, Tel Aviv University, Tel Aviv, Israel. [3]Department of Mathematics and Computer Science, The Open University of Israel, Raanana, Israel. [4]School of Psychological Sciences, Faculty of Social Sciences, Tel Aviv University, Tel Aviv, Israel. ✉email: igozes@tauex.tau.ac.il

Received: 13 September 2021 Revised: 21 April 2022 Accepted: 26 April 2022
Published online: 10 May 2022

MT assembly [20], growth cone formation [22], neurite outgrowth [22, 23] and dendritic spine maturation [19, 24].

A growing body of compelling data has linked MT-associated mutations to a variety of neurodevelopmental disorders, including ASD [25]. Accordingly, we previously reported that mutated ADNP affects MT dynamics and inhibits Tau-MT interactions [4, 13]. In turn, EB1/EB3 protein binding of NAP [20] protects against MT/Tau deficiencies induced by *ADNP* mutations in cell culture [4, 13] and in a mouse model carrying the most prevalent ADNP syndrome mutation [26]. In clinical trials involving amnestic patients with mild cognitive impairment exhibiting tauopathy, NAP administration led to increased cognitive scores [27].

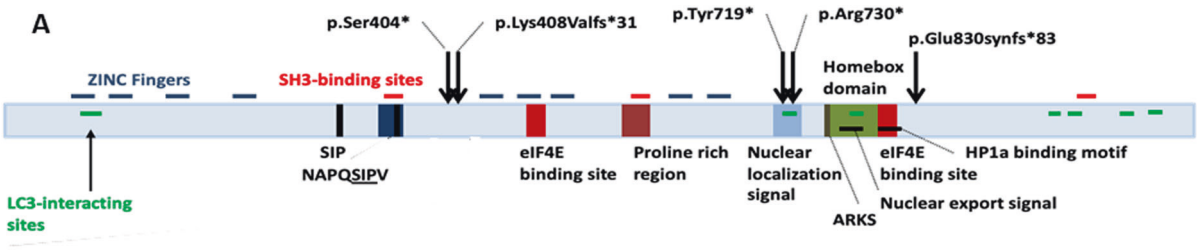

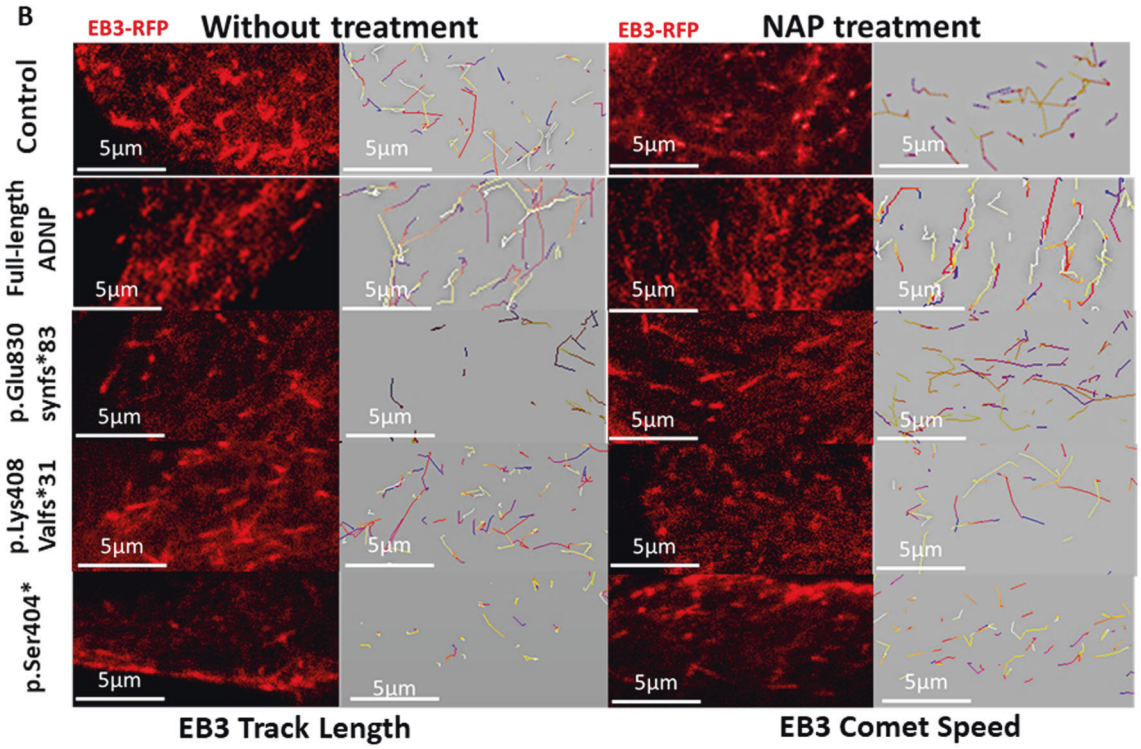

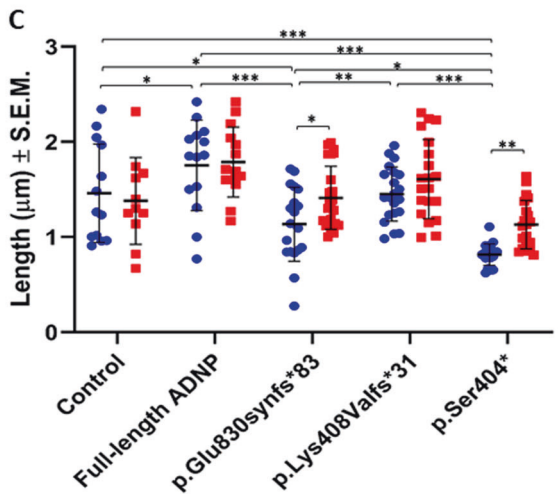

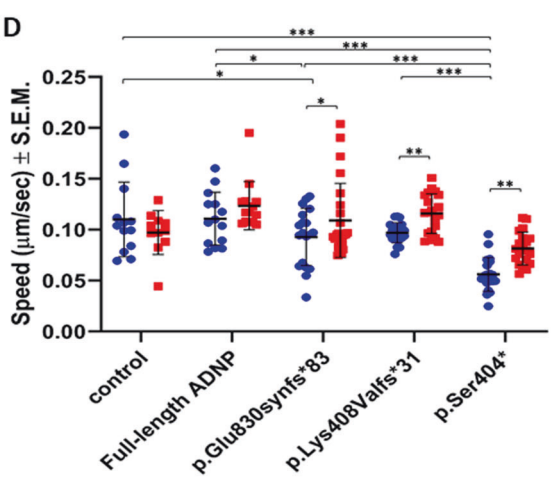

Fig. 1 Truncated ADNP proteins impair MT dynamics and assembly. A The locations of functional regions are depicted along the full-length human ADNP coding sequence, based on previously published findings [4, 6]. Arrows indicate mutated residues addressed here and previously [4, 13]. Selected SH3-binding sites are indicated by red lines (Table S1). **B** Captures of live imaging of differentiated N1E-115 cells expressing RFP-tagged EB3 protein and GFP-tagged full-length or truncated ADNP with or without NAP treatment (10^{-12}M, 4 h). Transfection with a backbone plasmid (pEGFP-C1) expressing non-conjugated GFP served as a control. Colored lines (gray squares) represent tracks of EB3 comet-like structures (obtained using Imaris software). **C**, **D** Graphs represent the means (±SEM) of EB3 comet track lengths and speeds, accordingly. Statistical analysis of the data was performed by one-way ANOVA, LSD (SPSS 23) and further analyzed according to Tukey, as indicated in the text. *$P < 0.05$; **$P < 0.01$; ***$P < 0.001$ (statistical analysis is provided in Table S4). Control $n = 13$; NAP $n = 11$; full-length ADNP $n = 14$; full-length ADNP + NAP $n = 14$; p.Glu830synfs*83 $n = 19$; p.Glu830synfs*83 + NAP $n = 24$; p.Lys408Valfs*31 $n = 21$; p.Lys408Valfs*31 + NAP $n = 20$; p.Ser404* $n = 20$; p.Ser404* + NAP $n = 20$.

Focusing on the cytoskeleton, the product of a major ASD and schizophrenia gene [28] termed Src homology 3 (SH3) and multiple ankyrin repeat domains protein 3 (SHANK3) interacts with the cytoskeleton through SH3 domain-ligand association [29] and an actin-binding site to modify dendritic spine morphology [30, 31]. The 1% of ASD patients presenting various mutations in *SHANK3* make it a high risk gene for monogenic ASD [32, 33]. SHANK3 is a critical protein in the post-synaptic density of glutamatergic neurons [32], acting as a scaffold protein that binds glutamate receptors to the cytoskeleton, and thus is essential for synaptic transmission and integrity [32–34]. The InsG3680 mouse carries a patient-derived frameshift-STOP *Shank3* mutation [28, 34] and exhibits major deficits in cortico-striatal synaptic transmission, with aberrant electrical activity, and autistic-like behavior [28].

While comparing effects of different ADNP mutations, we identified SH3-binding sites in the ADNP protein sequence and showed that these motifs play an instrumental role in ADNP-mediated regulation of MTs. We further identified an SH3-domain interacting ligand site in NAP (namely, NAPVSIP), enhancing Tau-MT interactions more effectively than the NAP-derived peptide SKIP [11, 35] that lacks the SH3-ligand-interaction motif. Lastly, we identified an actin-binding-site in ADNP and showed NAP-mediated protection against InsG3680-*Shank3*-induced deficits.

MATERIALS AND METHODS

Detailed methods

The Supplementary File provides additional methodological details.

Plasmid construction

Protein-expressing plasmids were constructed based on the pEGFP-C1 backbone plasmid, including those for full-length ADNP or the truncated ADNP proteins p.Glu830synfs*83, p.Lys408Valfs*31 or p.Ser404* [13]. The mutated *ADNP* cDNA sequences were derived from human patient lymphoblastoid cells [4, 13]. Protein expression was verified by fluorescent imaging and immunoblotting (Figs. S1, S2).

Cell differentiation, co-transfection of overexpression plasmids, live imaging, and fluorescence recovery after photobleaching (FRAP)

Mouse neuroblastoma N1E-115 cells were maintained as before [4]. Differentiated cells were transfected with the appropriate plasmids. Live imaging for MT dynamic assessments and FRAP for Tau-MT interaction analyses were performed as before with 10^{-12}M NAP [4, 13] or SKIP [36].

Mice

Homozygous InsG3680 *Shank3* male mice and littermate controls (wild type, WT) [28], were tested in two independent experimental groups. Group 1, comprising 6–40-week-old mice (11 *Shank3* and 7 WT), were treated with vehicle (5 µl, intranasal) for 3 days and then subjected to open field tests (50 × 50 cm white Plexiglas arena for 60 min.). Mouse movements were recorded using the EthoVision XT system (Noldus, Leesburg, VA) [37]. After another week of vehicle treatment and 2.5 weeks of daily NAP treatment (0.5 µg NAP/5 µl vehicle), the same animals were tested again in the open field (i.e., each mouse was tested twice, serving as its own control). Group 2 comprised 31–76-week-old mice objectively randomized into placebo and treatment groups of the same ages (10 male mice/experimental group, based on power calculations [38]). These mice received daily (5 days/week) intranasal NAP or vehicle for 1 month [24]. No blinding was necessary as unbiased video recording was implemented. Here, open field assessments (15 min) allowed for self-grooming detection using Behavioral Observation Research Interactive Software (BORIS). Social approach tests (three-chamber-social-recognition, Noldus) [37] measured the frequency and time spent exploring the mouse or cup, either directly or in the chamber where the mouse or empty cup alone were present. Experiments were approved by the institutional animal care and use committee of Tel Aviv University and the Israel Ministry of Health.

Co-immunoprecipitation (co-IP)

Co-IPs were performed as described [17]. Briefly, mouse monoclonal C4 antibodies to actin (10 µg; MP Biomedicals, Irvine, CA, cat No. 691001) were cross-linked with A/G PLUS-agarose beads (30 µl, co-IP kit, Thermo Fisher Scientific, Waltham, MA). An aliquot (1 mg) of proteins, extracted from Institute of Cancer Research (ICR) mouse hippocampus [24], were incubated with the antibodies (4 °C, 12 h). The soluble fraction was then halved and incubated with 3 mg NAPVSIPQ or 1.5 mg SKIP peptides [3, 20]. InsG3680-*Shank3* mouse brain extracts were subjected to co-IP with agarose-conjugated anti-β-actin antibodies (2A3, sc-517582, Santa Cruz, CA). Co-captured proteins were separated by 8% SDS-PAGE and analyzed by Western blotting. Primary antibodies included mouse monoclonal-actin (1:2000, ab3280, Abcam, Cambridge, UK), ADNP F9 (1:200, SC-376674, Santa Cruz, CA), and Tau (1:500, AHB0042), and rabbit polyclonal-SHANK3 (1:1000, OAPB01581, Aviva System Biology, San Diego, CA). Proteins were visualized with horseradish peroxidase-conjugated goat anti-mouse (1:5000, Jackson, Hamburg, Germany) or anti-rabbit (1:5000, Jackson) secondary antibodies and SuperSignal Chemiluminescent Substrates (Thermo Fisher Scientific).

ADNP/SHANK3/actin interactions in silico

I-TASSER (https://zhanggroup.org/I-TASSER) was used for protein structure modeling and Patchdock (https://bioinfo3d.cs.tau.ac.il/PatchDock/) was used for in silico protein/protein docking of ADNP, SHANK3, and actin. PyMOL software was used to create figures.

Statistical analysis

Data are presented as means ± S.E.M., with cell culture data representing the average of at least three independent experiments. Statistical analysis was performed using two-way ANOVA in SigmaPlot 11 (Systat Software, San Jose, CA) or one-way ANOVA in IBM SPSS 23 (IBM, Armonk, NY). Tukey post hoc tests were performed for all pairwise multiple comparisons. If only a trend was observed, the data were further analyzed less stringently (i.e., by an LSD post hoc test). For behavioral assessments, outlier values were excluded using the Grubbs test, and normal distribution was assessed.

RESULTS

Expression of ASD-associated truncated ADNP impairs EB3 activity at MT plus-ends, whereas NAP restores EB3 action

Different mutant versions of the ADNP protein (Fig. 1A) may have differential effects on MTs [4, 13]. To define the impact of these mutants on MTs, the products of five plasmids expressing backbone pEGFP-C1 and one of three truncated ADNP variants (p.Glu830synfs*83, p.Lys408Valfs*31, or p.Ser404*) or full-length ADNP (control) were compared in a mouse neuroblastoma N1E-115 cell model. ADNP p.Glu830synfs*83, which corresponds

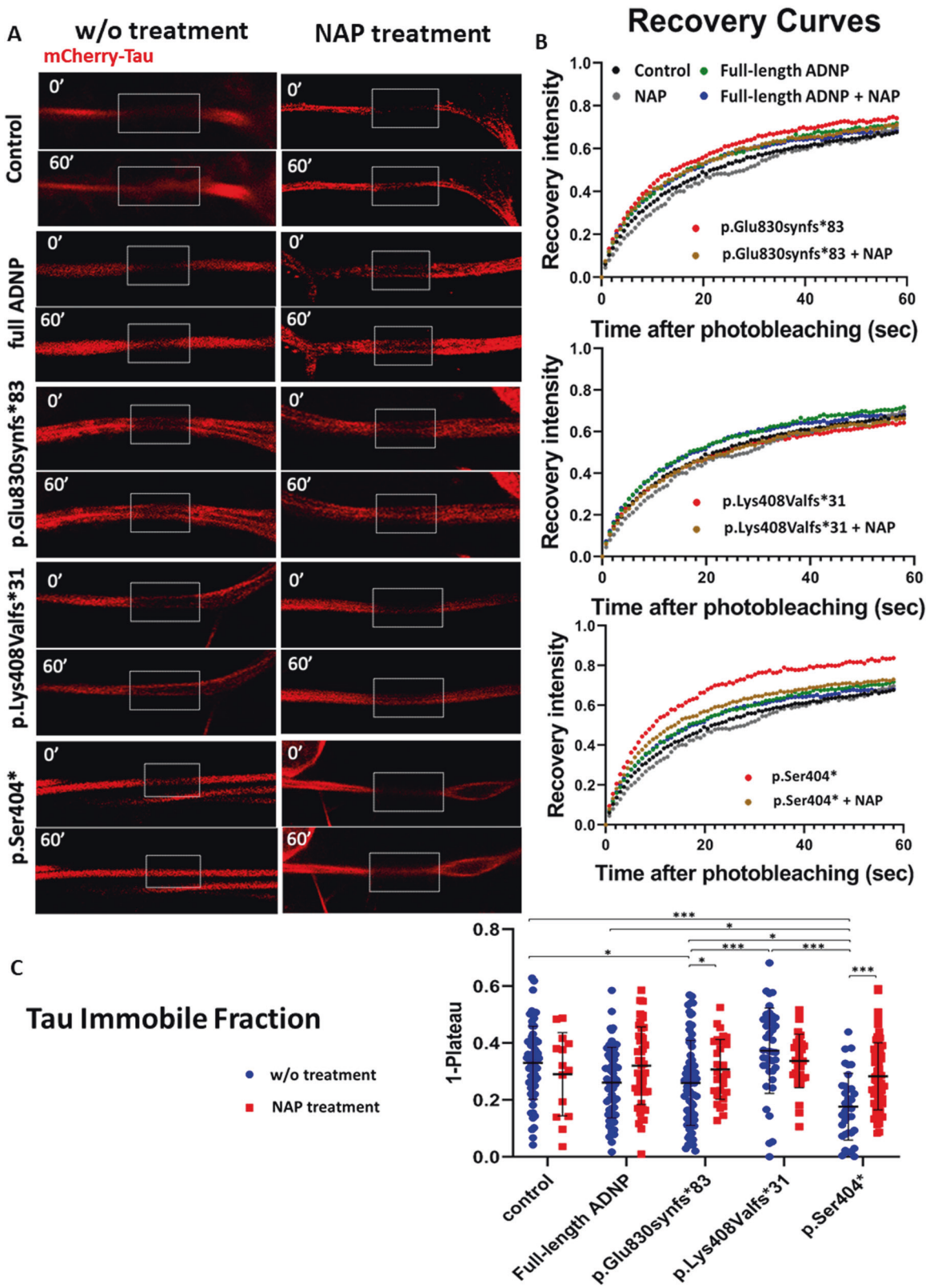

Fig. 2 Expression of truncated ADNP proteins reduces Tau-MT interactions. A Representative images of photobleaching (0′) and fluorescence recovery (60′) of mCherry-tagged Tau in differentiated N1E-115 cells co-transfected to express GFP-tagged full-length or truncated ADNP with or without NAP treatment (10^{-12}M, 4 h). Transfection with backbone plasmid (pEGFP-C1) expressing non-conjugated GFP served as a control. **B** FRAP recovery curves of normalized data (see Materials and Methods). **C** Means (±SEM) of the fitted data of immobile fractions from three independent experiments. Normalized FRAP data were fitted with one-exponential functions (GraphPad Prism 6) and statistical analysis was done by two-way ANOVA (SigmaPlot 11). *$P < 0.05$; ***$P < 0.001$; (Statistical analysis is shown in Table S4). Control $n = 64$; full-length ADNP $n = 55$; NAP $n = 14$; full-length ADNP + NAP $n = 46$; p.Glu830synfs*83 $n = 71$; p.Glu830synfs*83 + NAP $n = 25$; p.Lys408Valfs*31 $n = 36$; p.Lys408Valfs*31 + NAP $n = 35$; p.Ser404* $n = 33$; p.Ser404* + NAP $n = 62$.

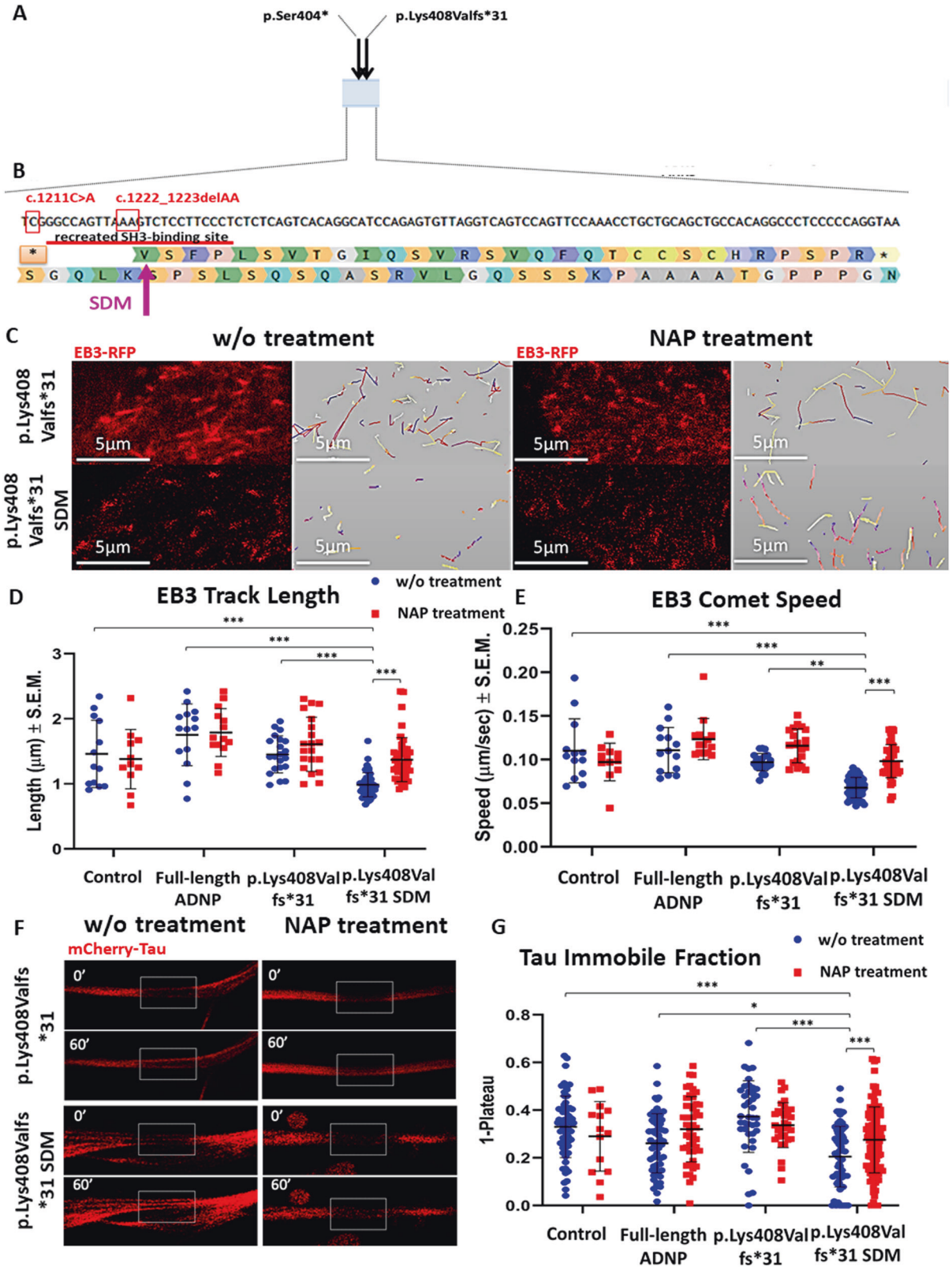

to most prevalent ADNP syndrome mutant [6] where the C-terminal portion of the protein is truncated (examined here for the first time), was compared with the two p.Lys408Valfs* and p.Ser404* mutants, both of which are truncated close to the N-terminal site.

To gauge the impacts of the different ADNP mutants on MT dynamics, time-lapse imaging of the comet-like structures formed by RFP-tagged EB3 proteins upon binding to MT plus-ends was next performed. The track lengths and track speeds of these EB3 comets reflect the lengths of newly growing MTs and the speeds

Fig. 3 ADNP p.Lys408Valfs*31 with a disrupted SH3-binding site exhibits adverse effects on MT dynamics and Tau-MT association. A The image presents part of Fig. 1A and is linked to (**B**). **B** Human ADNP cDNA (1210–1316 bp) and amino acid (404–439 residues) partial sequences. The cDNA sequence presents the locations of the c.1211C<A (p.Ser404*) and c.1222_1223delAA (p.Lys408Valfs*31) mutations. The upper amino acid sequence represents the frameshift sequence of the ADNP p.Lys4008Valfs*31 mutant, with the locations of stop codons in the coding sequence marked with asterisks. The lower amino acid sequence represents native ADNP. The red line indicates a predicted recreated SH3-binding site. The pink arrow depicts the site of site-directed-mutagenesis (SDM) that destroyed the recreated SH3-binding site. **C** Captures of time-lapse imaging, as described in the legend to Fig. 1. Representative images of truncated ADNP p.Lys408Valfs*31 (as in Fig. 1A) are presented for comparison with p. Lys408Valfs*31SDM in which the SH3-binding site was destroyed (Supplementary Fig. S3) with or without NAP treatment (10^{-12}M, 4 h). **D**, **E** Means (±SEM) of EB3 comet track lengths (**D**) and speeds (**E**). Data for the control and full-length and p.Lys408Valfs*31 ADNP are as in Fig. 1 and are presented here for comparison with p.Lys408Valfs*31 SDM (subjected to site-directed-mutagenesis abolishing the SH3-binding site. Statistical analysis was performed as described in the legend to Fig. 1. *$P < 0.05$; ***$P < 0.001$ (statistical analysis is provided in Table S4); p.Lys408Valfs*31 SDM $n = 45$; p.Lys408Valfs*31 SDM + NAP $n = 45$. **F** FRAP was performed as described in the legend to Fig. 2. Representative images of mCherry-tagged Tau photobleaching (0′) and fluorescence recovery (60′) of truncated ADNP p.Lys408Valfs*31 (as in Fig. 2A) are presented for comparison with p.Lys408Valfs*31SDM (subjected to site-directed-mutagenesis) with or without NAP treatment (10^{-12}M, 4 h). **G** Graph represents averages (±SEM) of the fitted data (from three independent experiments) of immobile Tau fractions. FRAP recovery curves of normalized data can be found in Supplementary Fig. S4. Statistical analysis was performed as described in the legend to Fig. 2. *$P < 0.05$; ***$P < 0.001$; p.Lys408Valfs*31 SDM $n = 66$; p.Lys408Valfs*31 SDM + NAP $n = 104$.

of MT assembly, respectively [20]. In addition to addressing how the ANDP mutants affected MT dynamics, we also considered whether addition of NAP (10^{-12}M for 4 h) could modulate these effects [4].

Overexpression of full-length ADNP significantly increased EB3 comet track lengths but had no impact on EB3 comet speed. NAP treatment had no additional effect (Fig. 1B–D) [4]. ADNP p.Ser404* significantly decreased EB3 comet track lengths, as compared to either full-length ADNP or empty plasmid, while ADNP p. Glu830synfs*83 caused a significant reduction of EB3 track lengths only in comparison to full-length ADNP (Fig. 1B, C). When considering EB3 comet speed, significant effects of ADNP p. Glu830synfs*83 and p.Ser404* were noted, relative to full-length ADNP and empty vector (Fig. 1D). Surprisingly, p.Lys408Valfs*31 ADNP had no impact on EB3 activity, as compared to either full-length ADNP or empty plasmid (Fig. 1B–D).

NAP treatment significantly augmented the speed and track length of the EB3 comets of p.Glu830synfs*83 and p.Ser404* mutants and comet speed of p.Lys408Valfs*31 (Fig. 1B–D). Notably, these results were obtained by the non-stringent LSD post hoc test, while analysis with a Tukey test showed significance only for those comparisons exhibiting LSD, ***$P < 0.001$. In short, ADNP p.Ser404* had the most impact (Fig. 1C, D), with NAP providing significant protection against the ADNP p.Ser404*-mediated decrease in comet speed (*$P < 0.05$, Tukey).

Expression of ASD-associated truncated ADNP proteins diminishes Tau association with MTs, whereas NAP restores Tau-MT interactions

We next examined the effects of the full-length and truncated versions of ADNP with or without NAP treatment on Tau-MT interaction by FRAP, using mCherry-tagged Tau protein in the N1E-115 cell model (Fig. 2A). The plateau of fluorescence recovery within a photo-bleached region of interest (ROI, marked by white squares in Fig. 2A) determines the immobile fractions of mCherry-Tau bleached molecules, which do not free binding sites on MTs for incoming non-bleached mCherry-Tau proteins and thus do not contribute to fluorescence recovery. Therefore, the immobile mCherry-Tau fraction reflects the rate of Tau association with MTs.

While overexpression of full-length ADNP and NAP treatment yielded results no different from the control (Fig. 2A–C), ADNP p. Ser404* expression significantly attenuated Tau association with MTs [13]. The effect of ADNP p.Glu830synfs*83 was significantly different only in comparison to the control and not to full-length ADNP (Fig. 2A–C). NAP treatment significantly increased Tau-MT interaction with the ADNP p.Glu830synfs*83 and p.Ser404* mutants. Furthermore, as with EB3 activity (Fig. 1B–D), ADNP p. Lys408Valfs*31 did not impair Tau-MT association (Fig. 2A–C).

The frameshift sequence of p.Lys408Valfs*31 contains an SH3-binding motif restoring ADNP MT-function

The finding that the ADNP p.Lys408Valsf*31 truncated mutant had no significant effect on MT assembly and Tau-MT interactions, unlike the other ADNP mutants in which upstream and downstream positions are affected, including the p.Ser404* [13] and p. Glu830synfs*83 mutants here, as well as the relatively prevalent ADNP p.Arg730* and p.Tyr719* mutants addressed in earlier work [4] (Fig. 1A), encouraged further investigation.

Computational analysis of the ADNP p.Lys408Valfs*31 frameshift C-terminal region, which differs from the p.Ser404* mutant (Fig. 3B), using the eukaryotic linear motif (Elm) prediction tool [39] revealed a newly created SH3-binding site, among other Elm-predicted motifs (Table S1). Protein-protein interactions mediated by SH3 domain-ligand association are involved in a wide variety of biological processes. In particular, the Tau protein SH3-binding site (Table S2) associates with Tau kinases to modulate Tau phosphorylation and MT interactions [40]. Thus, we considered whether the decreased impact of ADNP p.Lys408Valsf*31 expression on MT-Tau interactions and EB3 activity was mediated by the predicted SH3-binding site. Accordingly, we altered the SH3-binding site in the ADNP p.Lys408Valsf*31 plasmid by substitution of one nucleotide (p.Val408Leu*) using site-directed-mutagenesis (SDM), (Figs. S3, 3B). ADNP p.Lys408Valsf*31SDM expression coupled with live-cell imaging showed significant decreases in EB3 track lengths and comet speeds (compared to empty vector, full-length or p.Lys408Valsf*31, Fig. 3C–E). NAP treatment restored EB3 activity to control levels (Fig. 3C–E).

FRAP analysis revealed a significantly attenuated Tau immobile fraction following ADNP p.Lys408Valsf*31SDM expression, as compared to the control, full-length ADNP, and ADNP p. Lys408Valsf*31 (Figs. 3F, G, S4). Such attenuation was completely prevented by NAP treatment (Figs. 3F, G, S4).

The NAP SH3-binding motif increases NAP-mediated protection against Tau-MT disassociation

As indicated above, ELM analysis of the frameshift tail of ADNP p. Lys408Valfs*31 indicated an SH3-binding motif, with this structural motif being absent in p.Lys408Valfs*31 SDM (Fig. 4A, Table S1). Further ELM analysis of the NAP (NAPVSIPQ) sequence indicated an SH3-binding motif overlapping with the SIP-EB-binding site [19]. No such SH3-binding motif was identified within the EB-interacting SKIP peptide [11, 36, 41] (Fig. 4A, Table S1). Therefore, we compared the effects of NAP and SKIP on MT dynamics and Tau-MT interactions. Time-lapse imaging tracking the growth of individual MTs with RFP-tagged EB3 protein showed that added NAP and SKIP (10^{-12}M, 4 h) similarly increased EB3 track lengths and speeds, as compared to the control (Fig. 4B, C).

A

Amino-acid Sequence	Source	SH3-binding motif by Elm	Probability by Elm
S**GQLVSFP**LSVTGIQSVRSVQ FQTCCSCHRPSPR*	frameshift tail of p.Lys408Valfs*31	LIG_SH3_3	0.0317
SGQLLSFPLSVTGIQSVRSVQF QTCCSCHRPSPR*	frameshift tail of p.Lys408Valfs*31 with SDM	No recognition	
NAPVSIPQ	NAP peptide	LIG_SH3_3	0.0317
SKIP	SKIP peptide	No recognition	

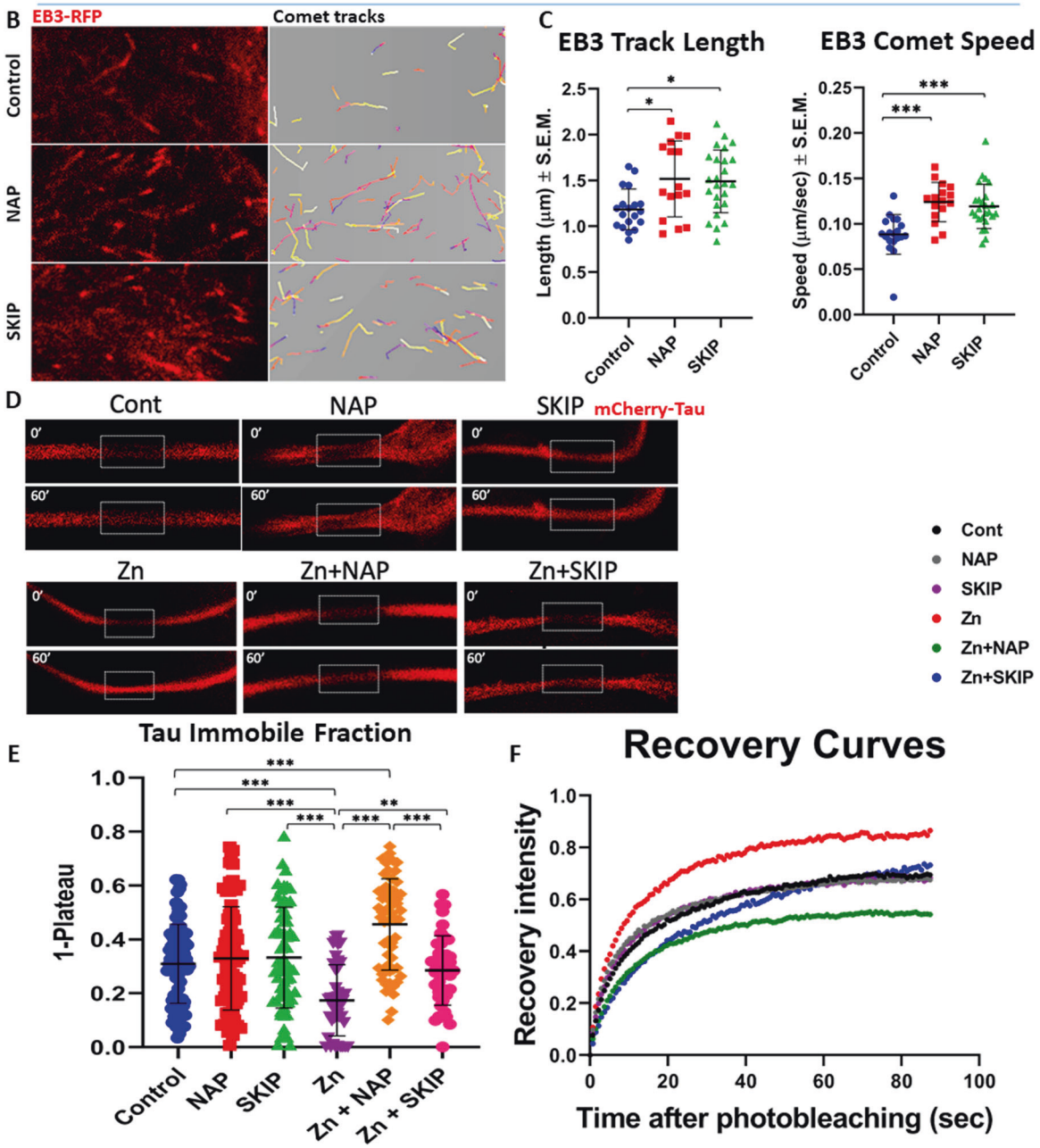

FRAP was performed to assess whether NAP and/or SKIP could maintain interactions of Tau with MTs in response to zinc, a Tau-MT dissociating agent [20, 22] (Fig. 4D–F). Extracellular zinc (400 μM, 1 h) significantly attenuated the MT-associated immobile Tau fraction, relative to non-treated control, whereas treatment with SKIP (10^{-12}M, 1 h) prevented the adverse effect of zinc (Fig. 4D–F). Exposure to zinc together with NAP (10^{-12}M, 1 h) increased Tau-MT interactions to a significantly higher extent than SKIP (Fig. 4D–F).

Fig. 4 The SH3-binding domain in NAP increases its protection against tauopathy so as to increase Tau-MT association. A SH3-binding sites (underlined), identified by Elm analysis, within different sequences. A complete list of Elm-predicted functional motifs is presented in Tables S1, S2. **B** Captures of time-lapse imaging tracking RFP-tagged EB3 protein in differentiated N1E-115 cells upon NAP or SKIP treatment (10^{-12}M, 4 h). Control—non-treated cells. Colored lines (gray squares) represent tracks of EB3 comet-like structures (obtained using Imaris software). **C** Graphs represent the averages (±SEM) of EB3 comet track lengths and speeds. Data from three independent experiments were collected in an unbiased fashion by Imaris software, and statistical analysis of the data was performed by one-way ANOVA (IBM SPSS 23). $^{*}P < 0.05$; $^{***}P < 0.001$; Control $n = 19$, NAP $n = 16$, SKIP $n = 25$. **D** FRAP. Representative images of mCherry-tagged Tau photobleaching (0′) and fluorescence recovery (60′) following zinc treatments (400 µM, 1 h) with or without NAP/SKIP (10^{-12}M, 1 h). **E** Graph represents averages (±SEM) of the fitted data of immobile fractions from three independent experiments. Statistical analysis was performed by one-way ANOVA (IBM SPSS 23). $^{**}P < 0.01$; $^{***}P < 0.001$, statistical analysis is provided in Table S4). Control $n = 82$; NAP $n = 73$; SKIP $n = 64$; Zn $n = 43$; Zn + NAP $n = 61$; Zn + SKIP $n = 44$. **F** FRAP recovery curves of normalized data (see Materials and methods).

ADNP and SHANK3 interact through SH3 and actin association

Given the newly discovered ADNP/NAP SH3-binding motif, we asked whether SH3 domain-containing SHANK3 also interacts with ADNP/NAP. For this, we performed further ELM analysis [39] on ADNP, SHANK3, Tau, EB1, and EB3 and predicted actin-binding sites in each of these proteins, as well as SH3 ligand-binding sites that interact with the SHANK3 SH3 domain (Table S2). Figure 5A depicts an in silico molecular interaction model of ADNP and SHANK3, highlighting the SHANK3-SH3-domain, the NAP-SH3-ligand site (responsible for direct ADNP-SHANK3 binding) and actin-binding sites on the two proteins. The insert zooms in on NAP interaction with the SHANK3 SH3 domain. Figure 5B compares and contrasts ADNP binding with a SHANK3 mutant (SHANK3-AOAOU1RR93-INSG3690). Interestingly, as can be observed in Fig. 5A1, B1, the actin-binding site is located differently in a WT SHANK3-ADNP complex and the mutant SHANK3INSG3690-ADNP complex, with SHANK3 conformation regulating actin binding [31]. Furthermore, inserts 5A2 and 5B2 show the different positions of NAP when bound to the SH3 domains of WT and mutant SHANK3. With these results in mind, we hypothesized that actin interacts differently with ADNP and SHANK3/mutated SHANK3, partly corrected by NAP but not by SKIP.

To test this hypothesis, we subjected hippocampal extracts from ICR mice to co-IP assays using actin antibodies in the presence of NAP or SKIP. We similarly probed brain extracts from InsG3680 *Shank3* mice [28] to test for Shank3, Tau and/or Adnp interactions with actin, including relevant controls. Figure 5C depicts hardly detectable actin-interacting Shank3-immunoreactivity in the ICR mouse hippocampus, although incubation with NAP yielded positive Shank3-immunoreactive band (E1, E2, E3, Fig. 5C, blue box and ellipse). In contrast, incubation with SKIP showed a diminished Shank3-like band, as compared to NAP treatment. Similar results were obtained when actin-Tau interactions were tested. Additional co-IP efforts using actin antibodies probed InsG3680 *Shank3* brain extracts Changes in mutant Shank3 interactions with actin upon NAP incubation were noted (Fig. 5D). To extend these findings, we compared WT and mutant Shank3-expressing InsG3680 mice treated with NAP in vivo (Fig. 5E). Actin antibody-interacting Shank3 and Adnp were captured at higher levels in brains of the latter group, with this increase being normalized by NAP treatment (Figs. 5G, F, S5).

NAP protects against the effects of InsG3680 Shank3 in a model of Phelan-McDermid autism syndrome

Given the apparent in vivo effect of NAP on mutant Shank3-expressing mice, open field behavior [41] measured anxiety in a group of mice first treated with vehicle and then with NAP (Fig. 5H). WT mice exposed to vehicle showed a considerable number of entries into the center zone over 1 h, whereas mice expressing mutant Shank3 visited the center zone some 50% less. In contrast, after a 2.5 week NAP treatment, all mice presented similar behaviors (Fig. 5I). Males were used, as these present a significant phenotype [28] and NAP regulates *Shank3* mRNA transcripts in *Adnp*-deficient male but not female brains [24].

A second group of mice were subjected to placebo-controlled drug tests measured anxiety, as well as autistic (grooming and social recognition) behaviors [37, 42] (Fig. 5J). Open field behavior assessment showed a dramatic reduction in time spent in the center, again indicative of anxious/depressive behavior. This reduction was significantly alleviated by NAP treatment (Fig. 5K).

Repetitive behavior, a key autistic feature, was evaluated by measuring grooming frequency and duration. Average grooming duration, calculated by the cumulative duration of grooming divided by the frequency of such behavior, indicated that sham-treated *Shank3* mice showed higher values than did their WT counterparts (Fig. 5L). The sham-treated mice also showed higher grooming frequency than did NAP-treated *Shank3* mice (Fig. 5M). A three-chamber social-recognition test measured the frequency of and time spent exploring the mouse or cup, either directly or in the chamber where the mouse or the empty cup alone were present. The results clearly showed the indifferent behavior of the WT littermates, as well as of mice expressing mutant Shank3, although sham-treated such mice exhibited a significant reduction in mouse exploration, i.e., autistic behavior. This was coupled to normalization of behavior in NAP-treated mice expressing mutant Shank3, with a significant preference for the mouse over the empty cup (Fig. 5N, O). In a previous study, such an experiment revealed autistic behavior in juvenile mice [28]. Here, this was extended to elderly mice and to demonstrate correction of such behavior by NAP.

Lastly, NAP was extensively studied in two unique models of the ADNP syndrome, haploinsufficiency (*Adnp*$^{+/-}$) [21, 24, 37, 41, 42] and Adnp p.Tyr718* (Tyr mice, carrying the most prevalent ADNP syndrome mutation) [26]. Table S3 shows similarities between the models, further attesting to ADNP/SHANK3 common pathways, holding future for drug development, and better understanding of ASD.

DISCUSSION

Here, we described SH3-ligand-binding sites impacting ADNP function and differentiating pathological mutations. We further connected ADNP to SHANK3 (SH3 domain protein), associating two leading ASD proteins linking MTs and actin microfilaments.

Cytoplasmic ADNP activity is strongly correlated with MT-associated processes. Mediated by direct interactions with EB1/EB3 proteins, ADNP/NAP facilitates neurite outgrowth [23] and post-synaptic density 95 protein (PSD-95) expression [19], thereby modulating dendritic plasticity and MT dynamics [20]. Here, we discovered that expression of all but one ASD-associated mutant ADNP proteins apparently impaired EB3 activity on MT plus-ends, reflecting MT dynamics and assembly, with NAP restoring EB3 activity to control levels [4, 13]. EB3 upregulation is essential for guiding MT-actin interactions during dendritic spine formation [43]. In turn, NAP shifts EB1/EB3 association from hetero- to homo-dimerization, accompanied by increased recruitment of EB3 to MTs [20]. Thus, the altered activities of the ADNP mutants may change EB3-mediated MT-actin coordination and affect proper dendritic spine formation.

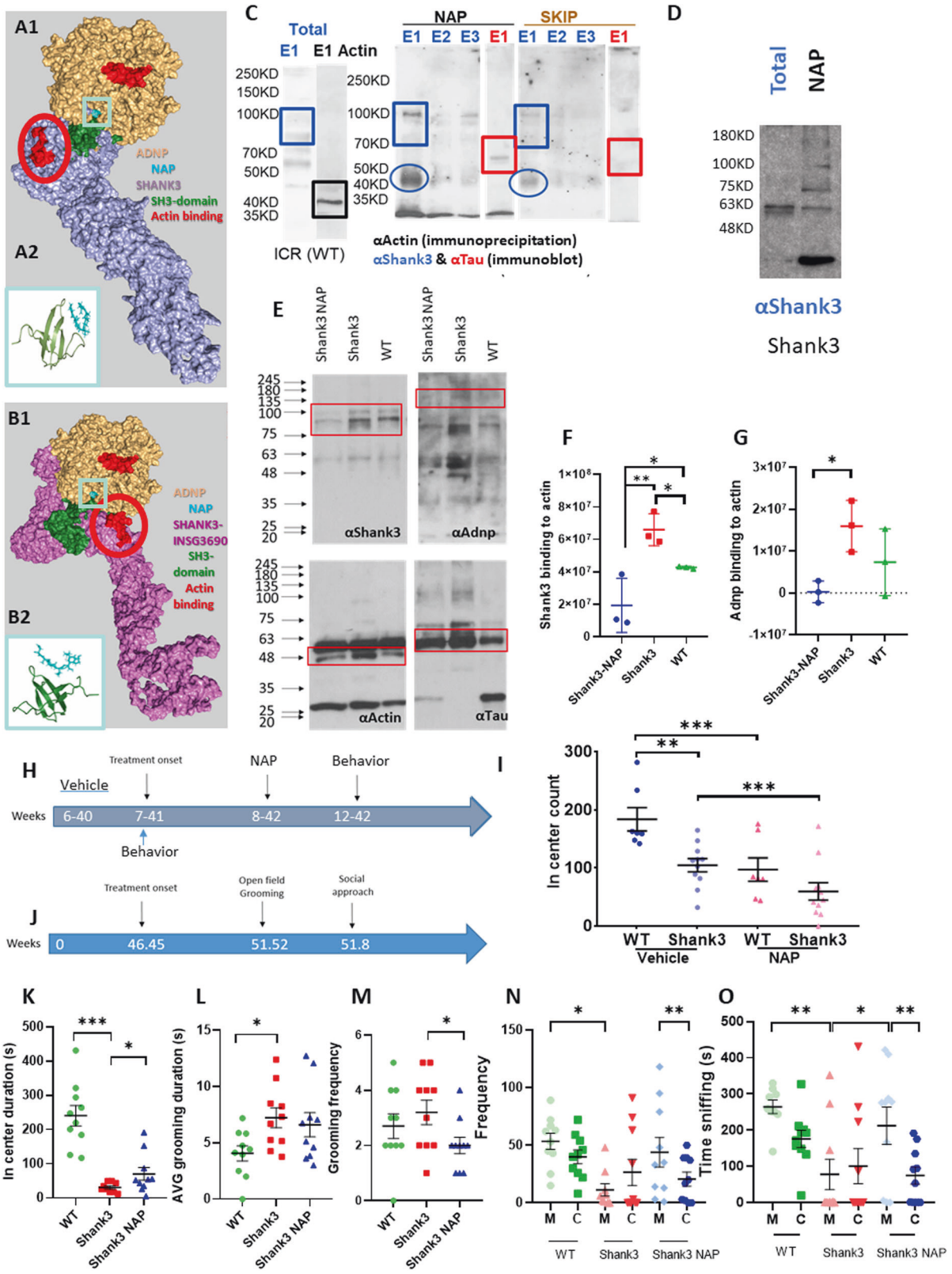

MT lattice-binding proteins also impact ASD neuropathology. For example, MT-associated protein 2 (MAP2) expression is reduced in the prefrontal cortex of adult ASD subjects [44]. Complementing this finding, ADNP deficiency results in MAP2 depletion [45] and NAP treatment restores MAP2 expression [23]. Deposition of Tau with a preponderance of the 4R isoform is associated with ASD [46]. Similarly, the ADNP syndrome exhibits tauopathy in post-mortem brains [13]. ADNP, as a member of the chromatin-remodeling complex SWI/SNF, impacts alternative splicing and correlates with Tau 3R expression [47]. Furthermore,

Fig. 5 In vitro and in vivo SHANK3/ADNP/NAP/actin interactions. A1-2, B1-2 Modeling of ADNP, SHANK3, and actin interactions. A1 Depicts WT SHANK3 (light blue) bound to ADNP (light orange). NAP (cyan) is shown within ADNP, while the SH3 domain (forest green) is part of SHANK3. The actin-binding sites in both ADNP and SHANK3 are colored red. The actin-binding site in SHANK3 was defined by Elm as LIG_Actin_WH2_2 (aa604–620), (http://elm.eu.org/), Table S2. A2 Is a zoom-in view of the interaction between NAP and the SHANK3-SH3 domain (A1). B1 And B2 depict the SHANK3-AOAOU1RR93-INSG3690 mutant (violet) bound to ADNP (light orange). All other protein motifs are color-coded as in (A1, A2). All protein structure building, i.e., ADNP (Uniprot ID: A0A669KBJ7; 1724 residues), SHANK3 N-terminal region (Uniprot ID: AOAOU1RR93; 1500 residues) and Shank3-AOAOU1RR93-INSG3690 (1287 residues) was performed using I-TASSER (https://zhanggroup.org/I-TASSER). Docking of ADNP to a SHANK3 SH3 domain model (PDB 6CPK, NMR structure) was performed using Patchdock https://bioinfo3d.cs.tau.ac.il/PatchDock/). NAP in ADNP and the SHANK3 SH3 domain locations are as per Table S2. Picture building used PyMOL software, and is shown using the SURFACE (A1, B1) or CARTOON modes (A2, B2). **C** Endogenous co-IP assay with ICR mouse hippocampus. To assess partner interaction enhancement, 3 mg NAP (NAPVSIPQ) or 1.5 mg SKIP (equimolar concentrations) were added to the affinity column flow through and the hippocampal extract was incubated with agarose-conjugated actin antibodies. Sequentially eluted fractions (E1, E2, E3) were further analyzed by immunoblotting with SHANK3 (blue) and Tau (red) antibodies. SHANK3/Tau–actin interactions in the brain extract were mostly seen in the presence of NAP but not with SKIP. **D** Brain extracts from *Shank3*-ASD-linked InsG3680 mutation mice [28] were subjected to co-IP with actin antibodies in the absence or presence of 3 mg NAP. **E** Co-IP assays of brain extracts from male mice (8–10 month old) with a *Shank3* ASD-linked InsG3680 mutation [28], objectively randomized and receiving daily intranasal treatment with 0.5 μg NAP or 5 μl vehicle or vehicle alone for 1 month [24]. Extracts (9 mice, three independent repeats; Fig. S5) were subjected to immunoprecipitation using actin antibodies. This identified ADNP (**F**) Shank3 and (**G**)/Adnp–actin association, which was apparently changed in the mutant mice and restored upon in vivo NAP treatment (red boxes denote the particular protein band). The different immunoreactive Shank3 bands are probably the result of tissue-specific alternative RNA splicing events [61], as well as cross-reactivity with other Shank family proteins members [62], with Shank3 [28], Adnp and NAP [24] regulating Shank2 expression in males. **H** Timeline of Group 1 (methods) *Shank3* mice first receiving the vehicle, followed by NAP. **I** Open field results of Group 1. Two-way repeated measures ANOVA was performed, significant genotype [$F(1,35) = 7.598$, $P = 0.014$], treatment [$F(1,35) = 53.45$, $P < 0.001$] and interaction, [$F(1,35) = 5.33$, $P = 0.035$] were revealed. **J** Timeline for Group 2 (WT $n = 10$, *Shank3* $n = 10$, *Shank3* NAP n = 10, methods), mouse ages are denoted in weeks. **K** NAP protected open field behavior against anxiety/depression in the *Shank3* mouse model (Mann–Whitney test, $^{***}P = < 0.001$ and $^{*}P = 0.037$). **L** Data followed by normal distribution were analyzed using two unpaired Student t-tests. Otherwise, the Mann–Whitney test was used. Data are expressed as means ± SEM. Genotype differences were found in the average grooming duration ($^{*}P = 0.0107$). **M** NAP reverses over-grooming frequency in *Shank3* mice ($^{*}P = 0.037$). **N**, **O** NAP improves social recognition in the *Shank3* mouse model. Two-way repeated measures ANOVA with group as the fixed factor and sniffed item (mouse vs. cup) as the repeated factor. The Tukey post hoc test was performed. Data are expressed as means ± SEM. **N** A main interaction effect was found [$F(2,27) = 4.165$, $P = 0.027$], with differences in mouse chamber frequency visits between sham-treated *Shank3* and WT mice ($^{*}P = 0.027$), and between mouse vs. cup frequency in the *Shank3* NAP group ($^{**}P = 0.005$). M-mouse, C-empty cup. ($^{*}P \le 0.05$; $^{**}P \le 0.01$). **O** Main effects for group [$F(2,27) = 4.067$, $P = 0.028$] and sniffed item [$F(1,28) = 5.621$, $P = 0.025$] were found, with significant difference in mouse sniffing times between sham-treated *Shank3* and WT mice ($^{**}P = 0.010$) and *Shank3* NAP-treated mice ($^{*}P = 0.036$). Significant differences were also noted between the time spent sniffing the cup and the mouse for *Shank3* NAP mice ($^{**}P = 0.005$). Data are expressed as means ± SEM. $^{*}P < 0.05$; $^{**}P < 0.01$; $^{***}P < 0.001$.

the SWI/SNF complex includes actin [9], while actin-dependent chromatin-remodeling plays a role in shaping the chromatin landscape and influences the regulation of genes involved in development and differentiation [48]. Here, we implied cytoplasmic actin/ADNP/NAP interactions that may affect chromatin function.

Regarding tauopathy, increased activity of the major Tau kinase glycogen synthase kinase-3β (GSK3β), accompanied with Tau hyper-phosphorylation, impairs social behavior [49]. As mentioned above, Adnp deficiency caused a tauopathy-like phenotype characterized by Tau hyper-phosphorylation and increased GSK3β activity, with cognitive deficiency. NAP treatment protected against these adverse features, while inhibiting Tau hyper-phosphorylation [21]. Here, we showed that truncated ADNP proteins (except for p.Lys408Valfs*31) decreased Tau-MT interactions and that NAP restored the association of Tau with MTs to control levels. These results are corroborated by our recent paper showing in vivo hyper-phosphorylated Tau-like tangles in the brains of Adnp p.Tyr718* mutant-expressing mice [26].

Our discovery of the spared ADNP truncating mutation having an additional SH3 ligand-binding site, emphasized the cross-talk among synapse sculpting proteins. SH3 domain-ligand cross-talk mediates protein-protein interactions in many signal transduction pathways and recruitment of SH3 domain-containing proteins directly or indirectly to appropriate substrates [50]. Binding to distinct SH3 ligands differently affects the structure and activity of SH3 domain-containing proteins [51, 52], including Fyn and PI3 kinases, which modulate Tau phosphorylation and Tau-MT interactions. Intriguingly, we discovered that ADNP includes SH3-binding sites and that the loss of these sites, as in the p.Glu830synfs*83 and p.Ser404* mutants, may partly explain the adverse impacts of the truncated ADNP variants on MT-associated proteins and MT-dependent cellular processes. Furthermore, we suggested that the observed moderate and non-significant effect of ADNP p.Lys408Valfs*31 stemmed from recreation of a SH3-binding site by frameshift, whereas experimentally destroying the SH3-binding had an adverse impact on MT dynamics and Tau-MT interactions. This was consistent with increased SH3-binding motif-mediated Tau recruitment to MTs upon NAP treatment, as opposed to what was seen upon treatment with SKIP, which lacks the SH3-binding site.

Our findings of protein interactions in the *Shank3* mutant autism model, as well as the modulation of these associations by NAP, further emphasizes the involvement of actin in ADNP/NAP/SHANK3 activities, culminating in behavioral outcomes, including autistic behaviors, as well as depression/anxiety. Future studies will assess NAP concentration and administration duration, in comparison to SKIP, also addressing spine plasticity (Table S2). These findings are important, given the existing psychiatric illness and regression in individuals with SHANK3/Phelan-McDermid syndrome [53], coupled with known NAP anxiolytic effects [54] and ADNP involvement in schizophrenia [3]. Mechanistically, we recognized tubulin [55] and actin [56] as key synaptic proteins, with SHANK-cortactin interactions controlling actin dynamics, maintaining the flexibilities of neuronal spines and synapses [57] and with ADNP NAP regulating dendritic spines [24]. Future studies should address how protein modifications, including the S-nitroso-proteome linked with SHANK3 mutants [58], emphasizing ADNP regulation by NO [59] and NAP regulation of NO formation [60], affect these relations.

In conclusion, our findings suggest that ASD-linked ADNP mutations impact interactions with multiple cytoskeletal-associated proteins, especially SHANK3, which in turn adversely affect downstream MT dynamics. This further hinders essential neuronal processes throughout early development into adulthood, triggering alone or partly contributing, in conjunction with nuclear ADNP activity, to ASD neuropathology. The current findings identify NAP as an SH3-ligand and EB1/3-associated

peptide [19, 20], providing another piece of the molecular mechanism explaining the protective activity of NAP. Importantly, this paves the path for using NAP (davunetide, CP201) as a drug prototype in cytoskeletal treatment against neurodegenerative or developmental diseases.

REFERENCES

1. Pinhasov A, Mandel S, Torchinsky A, Giladi E, Pittel Z, Goldsweig AM, et al. Activity-dependent neuroprotective protein: a novel gene essential for brain formation. Brain Res Dev Brain Res. 2003;144:83–90.
2. Mandel S, Rechavi G, Gozes I. Activity-dependent neuroprotective protein (ADNP) differentially interacts with chromatin to regulate genes essential for embryogenesis. Dev Biol. 2007;303:814–24.
3. Merenlender-Wagner A, Malishkevich A, Shemer Z, Udawela M, Gibbons A, Scarr E, et al. Autophagy has a key role in the pathophysiology of schizophrenia. Mol Psychiatry. 2015;20:126–32.
4. Ivashko-Pachima Y, Hadar A, Grigg I, Korenková V, Kapitansky O, Karmon G, et al. Discovery of autism/intellectual disability somatic mutations in Alzheimer's brains: mutated ADNP cytoskeletal impairments and repair as a case study. Mol Psychiatry. 2021;26:1619–33.
5. Helsmoortel C, Vulto-van Silfhout AT, Coe BP, Vandeweyer G, Rooms L, van den Ende J, et al. A SWI/SNF-related autism syndrome caused by de novo mutations in ADNP. Nat Genet. 2014;46:380–4.
6. Van Dijck A, Vulto-van Silfhout AT, Cappuyns E, van der Werf IM, Mancini GM, Tzschach A, et al. Clinical presentation of a complex neurodevelopmental disorder caused by mutations in ADNP. Biol Psychiatry. 2019;85:287–97.
7. Satterstrom FK, Kosmicki JA, Wang J, Breen MS, De Rubeis S, An JY, et al. Large-scale exome sequencing study implicates both developmental and functional changes in the neurobiology of autism. Cell. 2020;180:568–84.e23.
8. Iossifov I, O'Roak BJ, Sanders SJ, Ronemus M, Krumm N, Levy D, et al. The contribution of de novo coding mutations to autism spectrum disorder. Nature. 2014;515:216–21.
9. Mandel S, Gozes I. Activity-dependent neuroprotective protein constitutes a novel element in the SWI/SNF chromatin remodeling complex. J Biol Chem. 2007;282:34448–56.
10. Ostapcuk V, Mohn F, Carl SH, Basters A, Hess D, Iesmantavicius V, et al. Activity-dependent neuroprotective protein recruits HP1 and CHD4 to control lineage-specifying genes. Nature. 2018;557:739–43.
11. Amram N, Hacohen-Kleiman G, Sragovich S, Malishkevich A, Katz J, Touloumi O, et al. Sexual divergence in microtubule function: the novel intranasal microtubule targeting SKIP normalizes axonal transport and enhances memory. Mol Psychiatry. 2016;21:1467–76.
12. Gozes I, Van Dijck A, Hacohen-Kleiman G, Grigg I, Karmon G, Giladi E, et al. Premature primary tooth eruption in cognitive/motor-delayed ADNP-mutated children. Transl Psychiatry. 2017;7:e1166.
13. Grigg I, Ivashko-Pachima Y, Hait TA, Korenková V, Touloumi O, Lagoudaki R, et al. Tauopathy in the young autistic brain: novel biomarker and therapeutic target. Transl Psychiatry. 2020;10:228.
14. Sun X, Peng X, Cao Y, Zhou Y, Sun Y. ADNP promotes neural differentiation by modulating Wnt/beta-catenin signaling. Nat Commun. 2020;11:2984.
15. Yan Q, Wulfridge P, Doherty J, Fernandez-Luna JL, Real PJ, Tang HY, et al. Proximity labeling identifies a repertoire of site-specific R-loop modulators. Nat Commun. 2022;13:53.
16. Ferrari R, de Llobet Cucalon LI, Di Vona C, Le Dilly F, Vidal E, Lioutas A, et al. TFIIIC binding to Alu elements controls gene expression via chromatin looping and histone acetylation. Mol Cell. 2020;77:475–87.e11.
17. Hadar A, Kapitansky O, Ganaiem M, Sragovich S, Lobyntseva A, Giladi E, et al. Introducing ADNP and SIRT1 as new partners regulating microtubules and histone methylation. Mol Psychiatry. 2021;26:6550–61.
18. Markenscoff-Papadimitriou E, Binyameen F, Whalen S, Price J, Lim K, Ypsilanti AR, et al. Autism risk gene POGZ promotes chromatin accessibility and expression of clustered synaptic genes. Cell Rep. 2021;37:110089.
19. Oz S, Kapitansky O, Ivashco-Pachima Y, Malishkevich A, Giladi E, Skalka N, et al. The NAP motif of activity-dependent neuroprotective protein (ADNP) regulates dendritic spines through microtubule end binding proteins. Mol Psychiatry. 2014;19:1115–24.
20. Ivashko-Pachima Y, Sayas CL, Malishkevich A, Gozes I. ADNP/NAP dramatically increase microtubule end-binding protein-Tau interaction: a novel avenue for protection against tauopathy. Mol Psychiatry. 2017;22:1335–44.
21. Vulih-Shultzman I, Pinhasov A, Mandel S, Grigoriadis N, Touloumi O, Pittel Z, et al. Activity-dependent neuroprotective protein snippet NAP reduces tau hyperphosphorylation and enhances learning in a novel transgenic mouse model. J Pharmacol Exp Ther. 2007;323:438–49.
22. Oz S, Ivashko-Pachima Y, Gozes I. The ADNP derived peptide, NAP modulates the tubulin pool: implication for neurotrophic and neuroprotective activities. PloS ONE. 2012;7:e51458.
23. Smith-Swintosky VL, Gozes I, Brenneman DE, D'Andrea MR, Plata-Salaman CR. Activity-dependent neurotrophic factor-9 and NAP promote neurite outgrowth in rat hippocampal and cortical cultures. J Mol Neurosci. 2005;25:225–38.
24. Hacohen-Kleiman G, Sragovich S, Karmon G, Gao AYL, Grigg I, Pasmanik-Chor M, et al. Activity-dependent neuroprotective protein deficiency models synaptic and developmental phenotypes of autism-like syndrome. J Clin Investig. 2018;128:4956–69.
25. Lasser M, Tiber J, Lowery LA. The role of the microtubule cytoskeleton in neurodevelopmental disorders. Front Cell Neurosci. 2018;12:165.
26. Karmon G, Sragovich S, Hacohen-Kleiman G, Ben-Horin-Hazak I, Kasparek P, Schuster B, et al. Novel ADNP syndrome mice reveal dramatic sex-specific peripheral gene expression with brain synaptic and Tau pathologies. Biol Psychiatry. 2021:S0006-3223(21)01630-9. https://doi.org/10.1016/j.biopsych.2021.09.018. Online ahead of print.
27. Morimoto BH, Schmechel D, Hirman J, Blackwell A, Keith J, Gold M, et al. A double-blind, placebo-controlled, ascending-dose, randomized study to evaluate the safety, tolerability and effects on cognition of AL-108 after 12 weeks of intranasal administration in subjects with mild cognitive impairment. Dement Geriatr Cogn Disord. 2013;35:325–36.
28. Zhou Y, Kaiser T, Monteiro P, Zhang X, Van der Goes MS, Wang D, et al. Mice with Shank3 mutations associated with ASD and schizophrenia display both shared and distinct defects. Neuron. 2016;89:147–62.
29. Schlessinger J. SH2/SH3 signaling proteins. Curr Opin Genet Dev. 1994;4:25–30.
30. Durand CM, Perroy J, Loll F, Perrais D, Fagni L, Bourgeron T, et al. SHANK3 mutations identified in autism lead to modification of dendritic spine morphology via an actin-dependent mechanism. Mol Psychiatry. 2012;17:71–84.
31. Salomaa SI, Miihkinen M, Kremneva E, Paatero I, Lilja J, Jacquemet G, et al. SHANK3 conformation regulates direct actin binding and crosstalk with Rap1 signaling. Curr Biol. 2021;31:4956–70.e59.
32. Monteiro P, Feng G. SHANK proteins: roles at the synapse and in autism spectrum disorder. Nat Rev Neurosci. 2017;18:147–57.
33. Barak B, Feng G. Neurobiology of social behavior abnormalities in autism and Williams syndrome. Nat Neurosci. 2016;19:647–55.
34. Durand CM, Betancur C, Boeckers TM, Bockmann J, Chaste P, Fauchereau F, et al. Mutations in the gene encoding the synaptic scaffolding protein SHANK3 are associated with autism spectrum disorders. Nat Genet. 2007;39:25–7.
35. Ivashko-Pachima Y, Gozes I. A novel microtubule-Tau association enhancer and neuroprotective drug candidate: Ac-SKIP. Front Cell Neurosci. 2019;13:435.
36. Ivashko-Pachima Y, Maor-Nof M, Gozes I. NAP (davunetide) preferential interaction with dynamic 3-repeat Tau explains differential protection in selected tauopathies. PloS ONE. 2019;14:e0213666.
37. Sragovich S, Ziv Y, Vaisvaser S, Shomron N, Hendler T, Gozes I. The autism-mutated ADNP plays a key role in stress response. Transl Psychiatry. 2019;9:235.
38. Jaljuli I, Kafkafi N, Giladi E, Golani I, Gozes I, Chesler E, et al. Improving replicability using interaction with laboratories: a multi-lab experimental assessment. BioRXiv. 2021. https://doi.org/10.1101/2021.12.05.471264.
39. Dinkel H, Van Roey K, Michael S, Kumar M, Uyar B, Altenberg B, et al. ELM 2016-data update and new functionality of the eukaryotic linear motif resource. Nucleic Acids Res. 2016;44:D294–300.
40. Reynolds CH, Garwood CJ, Wray S, Price C, Kellie S, Perera T, et al. Phosphorylation regulates tau interactions with Src homology 3 domains of phosphatidylinositol 3-kinase, phospholipase Cgamma1, Grb2, and Src family kinases. J Biol Chem. 2008;283:18177–86.
41. Sragovich S, Amram N, Yeheskel A, Gozes I. VIP/PACAP-based drug development: the ADNP/NAP-derived mirror peptides SKIP and D-SKIP exhibit distinctive in vivo and in silico effects. Front Cell Neurosci. 2019;13:589.
42. Sragovich S, Malishkevich A, Piontkewitz Y, Giladi E, Touloumi O, Lagoudaki R, et al. The autism/neuroprotection-linked ADNP/NAP regulate the excitatory glutamatergic synapse. Transl Psychiatry. 2019;9:2.
43. Jaworski J, Hoogenraad CC, Akhmanova A. Microtubule plus-end tracking proteins in differentiated mammalian cells. Int J Biochem cell Biol. 2008;40:619–37.
44. Mukaetova-Ladinska EB, Arnold H, Jaros E, Perry R, Perry E. Depletion of MAP2 expression and laminar cytoarchitectonic changes in dorsolateral prefrontal cortex in adult autistic individuals. Neuropathol Appl Neurobiol. 2004;30:615–23.
45. Mandel S, Spivak-Pohis I, Gozes I. ADNP differential nucleus/cytoplasm localization in neurons suggests multiple roles in neuronal differentiation and maintenance. J Mol Neurosci. 2008;35:127–41.
46. Garbern JY, Neumann M, Trojanowski JQ, Lee VM, Feldman G, Norris JW, et al. A mutation affecting the sodium/proton exchanger, SLC9A6, causes mental retardation with tau deposition. Brain. 2010;133:1391–402.
47. Schirer Y, Malishkevich A, Ophir Y, Lewis J, Giladi E, Gozes I. Novel marker for the onset of frontotemporal dementia: early increase in activity-dependent neuroprotective protein (ADNP) in the face of Tau mutation. PloS ONE. 2014;9:e87383.

48. Mahmood SR, Xie X, Hosny El Said N, Venit T, Gunsalus KC, Percipalle P. beta-actin dependent chromatin remodeling mediates compartment level changes in 3D genome architecture. Nat Commun. 2021;12:5240.
49. Latapy C, Rioux V, Guitton MJ, Beaulieu JM. Selective deletion of forebrain glycogen synthase kinase 3beta reveals a central role in serotonin-sensitive anxiety and social behaviour. Philos Trans R Soc Lond Ser B Biol Sci. 2012;367:2460–74.
50. Bar-Sagi D, Rotin D, Batzer A, Mandiyan V, Schlessinger J. SH3 domains direct cellular localization of signaling molecules. Cell. 1993;74:83–91.
51. Teyra J, Huang H, Jain S, Guan X, Dong A, Liu Y, et al. Comprehensive analysis of the human SH3 domain family reveals a wide variety of non-canonical specificities. Structure. 2017;25:1598–610.e3.
52. Kurochkina N, Guha U. SH3 domains: modules of protein-protein interactions. Biophys Rev. 2013;5:29–39.
53. Kohlenberg TM, Trelles MP, McLarney B, Betancur C, Thurm A, Kolevzon A. Psychiatric illness and regression in individuals with Phelan-McDermid syndrome. J Neurodev Disord. 2020;12:7.
54. Alcalay RN, Giladi E, Pick CG, Gozes I. Intranasal administration of NAP, a neuroprotective peptide, decreases anxiety-like behavior in aging mice in the elevated plus maze. Neurosci Lett. 2004;361:128–31.
55. Zisapel N, Levi M, Gozes I. Tubulin: an integral protein of mammalian synaptic vesicle membranes. J Neurochem. 1980;34:26–32.
56. Hofstein R, Hershkowitz M, Gozes I, Samuel D. The characterization and phosphorylation of an actin-like protein in synaptosomal membranes. Biochim Biophys Acta. 1980;624:153–62.
57. MacGillavry HD, Kerr JM, Kassner J, Frost NA, Blanpied TA. Shank-cortactin interactions control actin dynamics to maintain flexibility of neuronal spines and synapses. Eur J Neurosci. 2016;43:179–93.
58. Amal H, Barak B, Bhat V, Gong G, Joughin BA, Wang X, et al. Shank3 mutation in a mouse model of autism leads to changes in the S-nitroso-proteome and affects key proteins involved in vesicle release and synaptic function. Mol Psychiatry. 2020;25:1835–48.
59. Cosgrave AS, McKay JS, Morris R, Quinn JP, Thippeswamy T. Nitric oxide regulates activity-dependent neuroprotective protein (ADNP) in the dentate gyrus of the rodent model of kainic acid-induced seizure. J Mol Neurosci. 2009;39:9–21.
60. Ashur-Fabian O, Giladi E, Furman S, Steingart RA, Wollman Y, Fridkin M, et al. Vasoactive intestinal peptide and related molecules induce nitrite accumulation in the extracellular milieu of rat cerebral cortical cultures. Neurosci Lett. 2001;307:167–70.
61. Wang X, Xu Q, Bey AL, Lee Y, Jiang YH. Transcriptional and functional complexity of Shank3 provides a molecular framework to understand the phenotypic heterogeneity of SHANK3 causing autism and Shank3 mutant mice. Mol Autism. 2014;5:30.
62. Lim S, Naisbitt S, Yoon J, Hwang JI, Suh PG, Sheng M, et al. Characterization of the Shank family of synaptic proteins. Multiple genes, alternative splicing, and differential expression in brain and development. J Biol Chem. 1999;274:29510–8.

ACKNOWLEDGEMENTS

We are grateful to Tal Barak and Elad Malikov for their diligent work with the mutant *Shank3* model mice and Prof. R. Frank Kooy for the ADNP patient-derived lymphoblastoid cell lines. This work was partially supported by grants to Prof. IG from the European Research Area Network (ERA-NET) Neuron ADNPinMED, Drs. Ronith and Armand Stemmer and Arthur Gerbi (French Friends of Tel Aviv University), Holly and Jonathan Strelzik (American Friends of Tel Aviv University) and Anne and Alex Cohen (Canadian Friends of Tel Aviv University). IG and BB are further supported by Sagol School of Neuroscience Interdisciplinary Partnership Grant (SNIP). IG is Director of the Elton Laboratory for Molecular Neuroendocrinology and the former first incumbent of the Lily and Avraham Gildor Chair for the Investigation of Growth Factors. This work is in partial fulfillment of Ph.D. thesis requirements at the Miriam and Sheldon G. Adelson Graduate School, Sackler Faculty of Medicine, Tel Aviv University (MG), who was also generously supported by a Neubauer Family Foundation Student Scholarship. This work is also in partial fulfillment of M.Sc. thesis requirements at the Miriam and Sheldon G. Adelson Graduate School (AL) and at the Sagol School of Neuroscience, Tel Aviv University (IB-H-H).

AUTHOR CONTRIBUTIONS

Together with IG, YI-P planned and performed all the cell culture experiments (Figs. 1–4), and wrote an initial, in depth, draft. MG performed biochemical experiments outlined in Fig. 5. IB-H-H performed animal behavior experiments. AL performed biochemical experiments outlined in Fig. 5. NB helped with the biochemical experiments. IF, GL, SSr, GK, and EG helped with all animal experiments. SSh performed in silico analyses (Fig. 5). Homozygous Shank3 ASD-linked InsG3680 mutated mice were housed and tested under the supervision of BB. IG orchestrated and supervised the entire project and wrote the paper with data analysis and editorial remarks from all contributing authors.

COMPETING INTERESTS

NAP (CP201, davunetide) use is under patent protection (US patent nos. US7960334, US8618043, and USWO2017130190A1) (IG), PCT/IL2020/051010 (IG) and provisional patent applications (IG inventor and contributing scientists, YI-P, MG, IB-H-H, SS, EG). Davunetide is exclusively licensed to ATED Therapeutics LTD (IG, Co-Founder and Chief Scientific Officer).

ADDITIONAL INFORMATION

Supplementary information The online version contains supplementary material available at https://doi.org/10.1038/s41380-022-01603-w.

Correspondence and requests for materials should be addressed to Illana Gozes.

Reprints and permission information is available at http://www.nature.com/reprints

Publisher's note Springer Nature remains neutral with regard to jurisdictional claims in published maps and institutional affiliations.